Received: 27 March 2016 | Revised: 1 February 2018 | Accepted: 6 February 2018
DOI: 10.1002/joc.5493

International Journal of Climatology RMetS

RESEARCH ARTICLE

An index of coastal thermal effects of El Niño Southern Oscillation on the Peruvian Upwelling Ecosystem

C. Quispe-Ccalluari[1] | J. Tam[1] | H. Demarcq[3] | A. Chamorro[1] | D. Espinoza-Morriberón[1] | C. Romero[1] | N. Dominguez[2] | J. Ramos[1] | R. Oliveros-Ramos[1]

[1]Laboratorio de Modelado Oceanográfico, Ecosistémico y del Cambio Climático (LMOECC), Instituto del Mar del Perú, Callao, Peru

[2]Laboratorio de Hidrofísica Marina (LHM), Instituto del Mar del Perú, Callao, Peru

[3]Institut de Recherche pour le Développement, UMR MARBEC (IRD, Ifremer, Université de Montpellier, CNRS), 34200 Sète, France

Correspondence
C. Quispe-Ccalluari, Laboratorio de Modelado Oceanográfico, Ecosistémico y del Cambio Climático (LMOECC), Instituto del Mar del Perú, Callao, Peru.
Email: cquispe@imarpe.gob.pe

The Peruvian Upwelling Ecosystem (PUE) is one of the most productive ecosystem in the world in terms of productivity and fish catches, partly because its geographical location is affected by remote physical processes, such as the interannual climate variability of the Equatorial Pacific Ocean (EPO), whose dominant signal is El Niño Southern Oscillation (ENSO). In order to assess the thermal effects of ENSO off Peru, a Peruvian Coastal Thermal Index (PCTI) was developed representing 87.7% of the total variation of the Sea Surface Temperature (SST) anomalies of the PUE. Between 1982 and 2014, the PCTI detected 12 warm periods and 16 cold periods in the PUE. PCTI had a linear trend component, a low frequency component and a noise component, with 1.5%, 94.5% and 4% contributions to the total variance, respectively. Wavelet analysis of PCTI showed significant peaks of variability between the years 1996 and 1999 between periods of 0.4 and 6 years. A regime shift in variance of PCTI was detected in 1999, with a lower variance between 1999 and 2014 than between 1982 and 1998, which agreed with the start of a cold phase of the Pacific Decadal Oscillation. The decrease of variance of the PCTI could be linked to an increase of the local winds associated with a higher intensity of the average state of South Pacific Anticyclone. This atmospheric change might have strengthened the coastal upwelling and counteracted the intensity of warm periods in the PUE. Finally, the comparison of different indexes allowed to detect four periods where neutral conditions occurred in the EPO while warm periods occurred in the PUE (1993, 2008, 2012 and 2014); and 1 period where a warm episode occurred in the EPO (2004–2005) while a neutral condition occurred in the PUE.

KEYWORDS
coastal index, ENSO, Equatorial Pacific Ocean, Peruvian Upwelling Ecosystem

1 | INTRODUCTION

El Niño Southern Oscillation (ENSO) is a coupled ocean–atmosphere process that fluctuates interannually between two opposite states: a warm phase (El Nino) and a cold phase (La Niña) (McPhaden, Zebiak, & Glantz, 2006) with important teleconnections and cascading effects worldwide (McPhaden, 2002; Rasmusson & Carpenter, 1982; Trenberth, Branstator, Karoly, & Kumar, 1998). In fact, NOAA (2003) has defined El Niño (EN) and La Niña (LN) episodes, based on the Oceanic Niño Index (ONI). ONI is calculated as a 3 month running average of Sea Surface Temperature (SST) anomalies (SSTA) in the Niño 3.4 region (120°–170°W, 5°N–5°S) of Equatorial Pacific Ocean (EPO).

Recent studies have shown two types of EN episodes that can be distinguished based on the location of the maximum SSTA: (a) the Eastern Tropical Pacific EN (EP El Niño) and the Central Tropical Pacific EN (CP El Niño) (Capotondi et al., 2015; U.S. CLIVAR Report, 2013). This two types of EN episodes have different characteristics in their origin and development mechanisms (Kao & Yu, 2009; Kug, Jin, & An, 2009). Takahashi, Montecinos, Goubanova, and Dewitte (2011) introduced some indices that distinguished cold and moderate warm episodes in the Central Equatorial Pacific, and extreme warm episodes in the Eastern Equatorial Pacific. Furthermore, Yu and Kim (2013) identified a third scenario, called the Mixed type, where both EP El Niño and CP El Niño coexist.

ENSO has also numerous teleconnections worldwide, mostly associated to the North Pacific Gyre Oscillation dynamics (NPGO), driven by the atmospheric variability in the North Pacific. The NPGO capture the decadal expression of CP El Niño in the extratropical regions, much as the Pacific Decadal Oscillation (PDO) captures the low frequency expression of EP El Niño (Di Lorenzo et al., 2013). Several studies showed that the frequency of CP El Niño has increased in recent decades (Kao & Yu, 2009; Kug et al., 2009; Lee & McPhaden, 2010; Takahashi et al., 2011).

In addition, climate models have projected an increase in the frequency of extreme EN episodes due to global warming (Cai et al., 2014). On the other hand, since 2002, a recent hiatus in global warming, associated to a La Niña-like decadal cooling, may have decreased the intensity of EN episodes (Kosaka & Xie, 2013).

The Peruvian Upwelling Ecosystem (PUE) is one of the most productive ecosystem in the world in terms of fish catches and is strongly impacted by ENSO phases (Chavez, Bertrand, Guevara-Carrasco, Soler, & Csirke, 2008). The PUE has important linkages with local and regional processes. Locally, within approximately 100 km off the coast, the PUE is characterized by the coastal upwelling, which is influenced by local alongshore winds and Trade winds (Bakun, 1990). The coastal upwelling brings to surface, subsurface cold, nutrient-rich waters, triggering a high productivity which supports the largest anchovy fishery of the world (Chavez et al., 2008; Pennington et al., 2006; Zuta & Guillén, 1970). Nearshore waters are cold also because a quasi-permanent low-level stratus cloud deck inhibits solar radiation reaching the ocean surface (Amador, Alfaro, Lizano, & Magaña, 2006; Klein & Hartmann, 1993). Regionally, it is known that the two main physical effects of EN episodes on the PUE are: (a) an anomalous increase of the coastal SST, and (b) an anomalous deepening of the thermocline off the Peruvian coast, associated to a decrease in nutrients (Arntz & Fahrbach, 1996; Barber & Chavez, 1983). On the other hand, the main effects of LN episodes over the PUE are: a shallower thermocline, colder coastal temperatures, and increase in nutrients, compared to normal years (Xu, Chaia, Ñiquen, & Chavez, 2013). Thus, we use the term "thermal effects" to refer to anomalous changes in SST in the PUE caused by EN and LN episodes.

Furthermore, the PUE has linkages with non ENSO related climate variability, for instance, decadal variability (warm and cold regimes) associated to anchovy and sardine alternations (Chavez, Ryan, Lluch-Cota, & Ñiquen, 2003); the South Pacific Anticyclone (SPA), an important atmospheric structure located in the subtropical area that drives alongshore winds in the whole Humboldt Current System (Rahn & Garreaud, 2014); subseasonal activity originating from remote equatorial forcing, that is, downwelling and upwelling Kelvin waves (Belmadani, Echevin, Dewitte, & Colas, 2012; Camayo & Campos, 2006; Illig et al., 2014); and climate change would generate a moderate decrease of upwelling rates off Peru (Echevin, Goubanova, Belmadani, & Dewitte, 2012).

ENSO diversity has generated different impacts on the PUE. For instance, during the 1997–1998 EN, considered as a strong EP El Niño (Karnauskas, 2013; Yu & Kim, 2013), the warm pool displacement reached the Peruvian waters (Colas, Capet, McWilliams, & Shchepetkin, 2008); while during the 2004–2005 EN, considered as a CP El Niño (Dewitte et al., 2012; Yu & Kim, 2013), cold conditions remained off Peru (Dewitte et al., 2012).

The thermal effects of EN episodes on PUE can be counteracted by several factors and feedbacks, such as the intensification of upwelling-favourable winds driven by the SPA (Rahn & Garreaud, 2014). In fact, 1994–1995 (Karnauskas, 2013) and 2004–2005 (Dewitte et al., 2012) EN episodes were detected by ONI, while weak eastern Pacific SST anomalies were recorded and cold conditions remained off Peru during both periods.

On the other hand, local factors can generate warm periods in PUE without the remote equatorial forcing, such as the historical warm period which occurred in 1925 in PUE (Takahashi & Martinez, 2017), during a probable neutral state of ONI. In fact, an exceptional coastal warm period occurred during the austral summer-autumn seasons of 2017 in PUE, while a transition from LN episode to a neutral phase was occurring in EPO according to ONI (ENFEN, 2017; Ramírez & Briones, 2017).

As there have been important differences in the thermal conditions between the PUE and the EPO, there is a need to develop a suitable and representative index for the detection and forecasting of warm and cold periods off Peru, so the objective of this work is to develop and analyse an index of the coastal thermal effects of ENSO on the PUE. This paper is organized as follows: section 2 describes details about data and methods. The results are presented and discussed in section 3 and section 4, respectively. Finally, conclusions and recommendations are given in section 5.

2 | DATA AND METHODS

2.1 | Data

OISST (Optimum Interpolation Sea Surface Temperature) version2 obtained from the NOAA NCDC (National Climatic Data Center of the National Oceanic and Atmospheric Administration). The period covered was 1982–2014, with a spatial resolution of 0.25° and monthly averaged (Reynolds et al., 2007).

ONI, representative of the EPO obtained from NOAA CPC (Climate Prediction Center) (NOAA, 2015) for the same period.

Smoothed Niño 1 + 2 index (called here SN1 + 2), was calculated as the 3 month running average of Niño 1 + 2 index (N1 + 2). N1 + 2 comprises the area between 80°–90°W, 0°N–10°S in the Tropical Pacific Ocean, based on a 2° grid data of the Extended Reconstruction of Historical Sea Surface Temperature version 3b (ERSSTv3b; Smith, Reynolds, Peterson, & Lawrimore, 2008) and was obtained from NOAA CPC (Climate Prediction Center) (NOAA, 2015) for the same period.

Thermocline depth off Peru (called here Z15) is the depth of the 15 °C isotherm obtained from IMARPE, details about its calculations can be found in Espinoza-Morriberón et al. (2017). The period covered was 1982–2008.

2.2 | Methods

The study area was a coastal band located between 5°–19°S and 90°–70°W (Figure 1), representative of the PUE. The boundary of the upwelling area was defined as the maximum zonal gradient of the annual SST, which determine a thermal front between coastal and oceanic waters. The SSTA was calculated by removing the mean annual cycle of the 1982–2010 SST series.

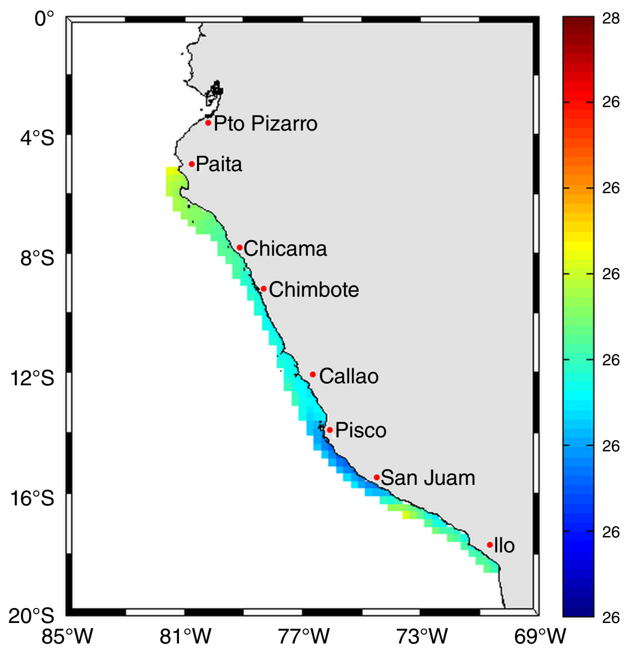

FIGURE 1 SST in the Peruvian Upwelling Ecosystem (PUE) from 1982 to 2014 [Colour figure can be viewed at wileyonlinelibrary.com]

The Peruvian Coastal Thermal Index (PCTI) was calculated as a 3 month running average of the first normalized principal component (PC) of the SSTA in the coastal zone. Singular value decomposition (SVD) was used to obtain the PC time series and EOF maps of the SSTA matrix. The PCTI was categorized into three conditions: cold (<−0.6), neutral (−0.6 a 0.4) and warm (>0.4). The PCTI has to persist at least three consecutive months over/under the thresholds to be categorized as a warm/cold period.

Several tools of time series analysis were used to analyse the PCTI in the time and frequency domains: robust regression analysis to remove the linear trend (Venables & Ripley, 2002), spectral analysis to identify frequencies with greater variability (Chatfield, 1996), Fourier filters to decompose signals from detrended PCTI (Emery & Thomson, 2004), wavelet analysis to detect time-frequency variations (Liu, Liang, & Weisberg, 2007; Torrence & Compo, 1998), sequential analysis to detect regime shift (Rodionov, 2004) and finally cross-correlation between PCTI and ONI to explore the lags (Venables & Ripley, 2002). The data analysis was performed using the R statistical software (R Core Team, 2016).

3 | RESULTS

3.1 | Temporal and spatial variations of the PCTI

The PCTI explained 87.7% of variability of the data, and was able to detect the thermal effects of the main EN episodes in 1986–1987, 1992–1993 and 1997–1998 in the PUE (Figure 2). On the other hand, the PCTI was also able to detect the thermal effects of the main LN episodes in 1988–1989 and 1999–2000. The frequency distribution of the PCTI showed a positive asymmetry, due to the occurrence of a few high temperatures caused by EN episodes (Figure 3).

The PCTI detected 12 warm periods in the PUE between 1982 and 2014 (Table 1). The five more intense warm periods were: from September 1982 to September 1983 with a peak of +4.6 (effect of EN 1982–1983 episode), from December 1986 to November 1987 with a peak of +1.51 (effect of EN 1986–1987 episode), from September 1991 to June 1992 with a peak of +2.27 (effect of EN 1991–1992 episode), from March 1997 to June 1998 with a peak of +3.2 (effect of EN 1997–1998 episode) and from May 2014 to July 2014 with a peak of +1.27.

The PCTI detected 16 cold periods in the PUE between 1982 and 2014 (Table 2). The five more intense cold periods were: from February 1982 to April 1982, from February 1984 to June 1986 with a minimum value of −1.04 (effect of LN 1984–1985 episode), from June to

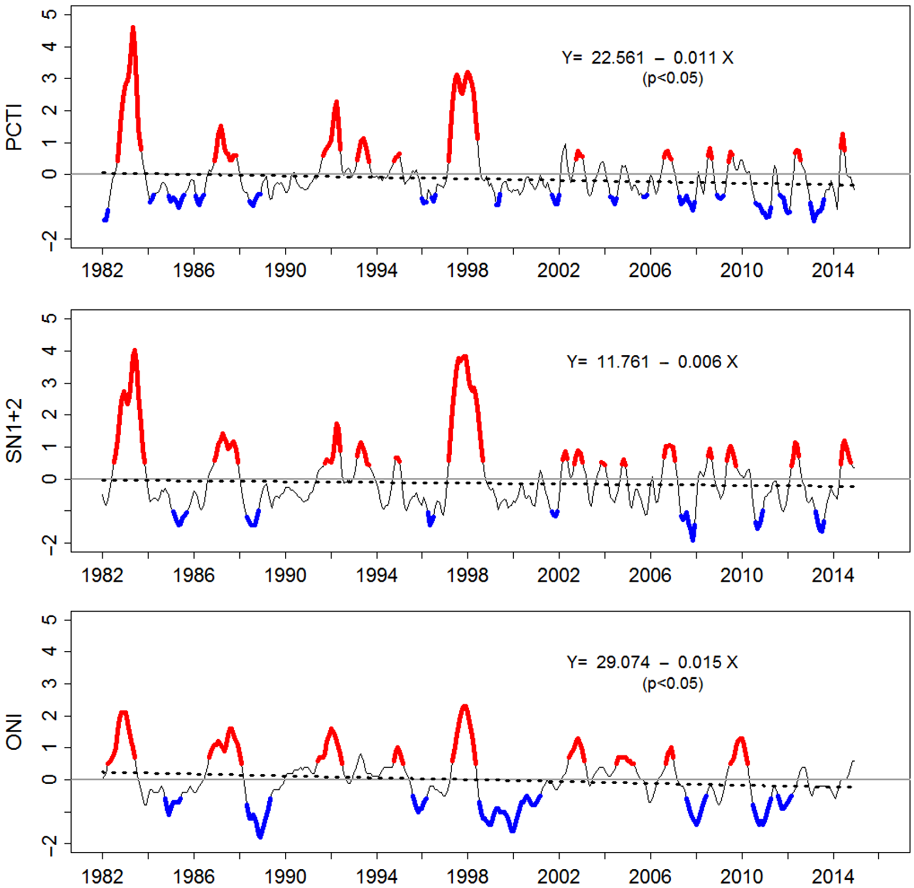

FIGURE 2 Monthly time series of PCTI, SN1 + 2, ONI and linear trend (thick dashed line) from 1982 to 2014 [Colour figure can be viewed at wileyonlinelibrary.com]

December 1988 with −0.96 (effect of LN 1988–1989 episode), from August 2010 to April 2011 with −1.34 (effect of LN 2010–2011 episode), from January to August 2013 with −1.44 (neutral period in the EPO).

The spatial structure of the PCTI, that is, the first EOF (87.7%) of the SSTA is shown in Figure 4. The PCTI displayed a large positive pattern in the Northern and Central Peru.

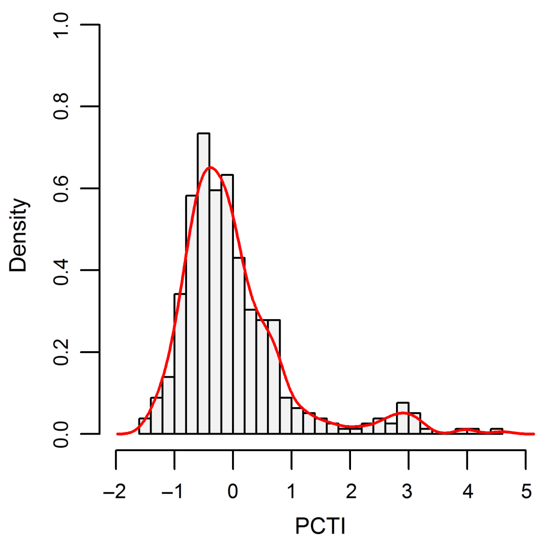

FIGURE 3 Frequency distribution of PCTI from 1982 to 2014 [Colour figure can be viewed at wileyonlinelibrary.com]

3.2 | Spectral frequencies of the PCTI

The PCTI presented a significant linear trend of −0.132 year^{-1} ($p < .05$). A spectral analysis of the detrended PCTI, and it exhibited six peaks of maximum variability at periods of 1.5, 2.1, 3, 3.7, 4.7 and 5.5 years (Figure 5). The PCTI was decomposed into three components: a linear trend component (Figure 2a), a large periods component (periods higher than 1.5 years) (Figure 6a) and a noise component (periods lower than 1.5 years) (Figure 6b). The contributions to the total variance of three components were: 1.5%

TABLE 1 Warm periods of PCTI from 1982 to 2014

N°	Periods	Maximum value PCTI	Duration (months)
1	September 1982 to September 1983	4.6	13
2	December 1986 to November 1987	1.51	12
3	September 1991 to June 1992	2.27	10
4	March 1993 to September 1993	1.12	7
5	October 1994 to January 1995	0.65	4
6	March 1997 to June 1998	3.2	16
7	October 2002 to January 2003	0.73	4
8	August 2006 to December 2006	0.75	5
9	July 2008 to September 2008	0.83	3
10	June 2009 to August 2009	0.72	3
11	May 2012 to August 2012	0.77	4
12	May 2014 to July 2014	1.27	3

TABLE 2 Cold periods of PCTI from 1982 to 2014

N°	Periods	Minimum value PCTI	Duration (months)
1	February 1982 to April 1982	−1.41	3
2	February 1984 to April 1984	−0.87	3
3	December 1984 to August 1985	−1.04	9
4	February 1986 to June 1986	−0.95	5
5	June 1988 to December 1988	−0.96	7
6	January 1996 to March 1996	−0.9	3
7	June 1996 to August 1996	−0.84	3
8	April 1999 to June 1999	−0.94	3
9	September 2001 to January 2002	−0.92	5
10	April 2004 to July 2004	−0.92	4
11	September 2005 to November 2005	−0.7	3
12	April 2007 to December 2007	−1.11	9
13	December 2008 to March 2009	−0.75	4
14	August 2010 to April 2011	−1.34	9
15	September 2011 to February 2012	−1.2	6
16	January 2013 to August 2013	−1.44	8

(linear component), 94.5% (high periods component) and 4% (noise component).

A wavelet analysis (Figure 7) showed the greatest variability in periods between 0.4 and 6 years, with a significant peak between 1996–1999, and minor peaks in periods between 0.4 to 2 years, during 1992–1993, 1997–1998, 2002–2003 and 2006–2007. In addition, a band of high variability was observed in periods of 4–6 years between 1990 and 2002.

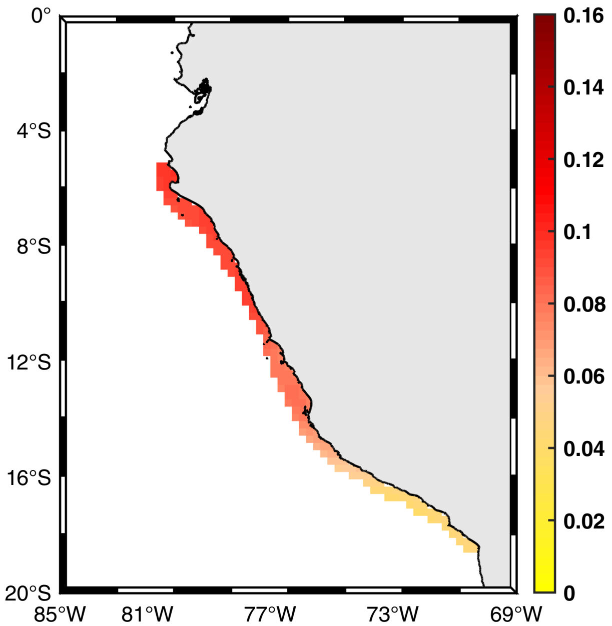

FIGURE 4 First EOF of sea surface temperature anomalies in the Peruvian Upwelling Ecosystem from 1982 to 2014 [Colour figure can be viewed at wileyonlinelibrary.com]

3.3 | Regime shift in the PCTI

Although the time series of the PCTI is relatively short (33 years), a sequential analysis based on the algorithm of Rodionov (2004) was performed by using annual averages. The algorithm was applied to detect possible shifts in both the mean and the variance, after the PCTI was detrended with robust regression. The analysis did not detect any changes in the mean, but detected a significant shift regime in the variance in 1999 (Figure 8) with a higher variance in the 1982–1998 regime, and lower variance in the 1999–2014 regime.

3.4 | Comparison of the PCTI with other indexes

The PCTI was compared to other indexes, such as ONI and SN1 + 2, during the study period (1982–2014) (Tables 3 and 4), by identifying warm and cold periods in the three time series. The same approach was used for ONI and SN1 + 2 (Table 5).

According to the ONI (Table 3), nine EN episodes and six LN episodes occurred in the EPO, meanwhile according to PCTI (Table 4), 12 warm periods and 12 cold periods occurred in the PUE. On the other hand, according to the SN1 + 2 index (Table 5), fourteen warm periods and seven cold periods occurred in the region Niño 1 + 2.

Comparison of indexes revealed five cases where the ONI and the PCTI did not match (Table 3). In four periods, ONI presented neutral conditions while, PCTI presented warm conditions (March–September 1993, July–September 2008, May–August 2012 and May–July 2014), and in one period ONI presented a warm condition (Jul 2004 to April 2005) while PCTI presented a neutral condition.

Based on the ONI variability during the study period, 15 significant episodes (EN and LN) occurred in 33 years (Table 3), while according to the PCTI variability 24 significant cold and warm periods occurred during the study period, that is, 60% higher. More interestingly, the ratio between the PCTI and the SN1 + 2 warm and cold events is 24/21 (Table 4), that is, a 14% higher.

Cross-correlation between PCTI and ONI (Figure 9) showed a lag in which ONI precedes PCTI of 1 month, with a Pearson correlation coefficient of 0.69 ($p < .05$).

ONI detected six LN episodes, while PCTI also detected cold periods, during the study period. However, the SN1 + 2 index detected five cold periods and one neutral period, probably because the SN1 + 2 is more influenced by the EPO than the more coastal PCTI, that better represents PUE conditions.

In addition, in order to investigate the subsurface ENSO variability along the coast, a correlation between the anomalies of Z15 off Peru and PCTI was performed (Figure 11), and a significant correlation of +0.85 was found, indicating that an anomalous increase (decrease) of the thermocline

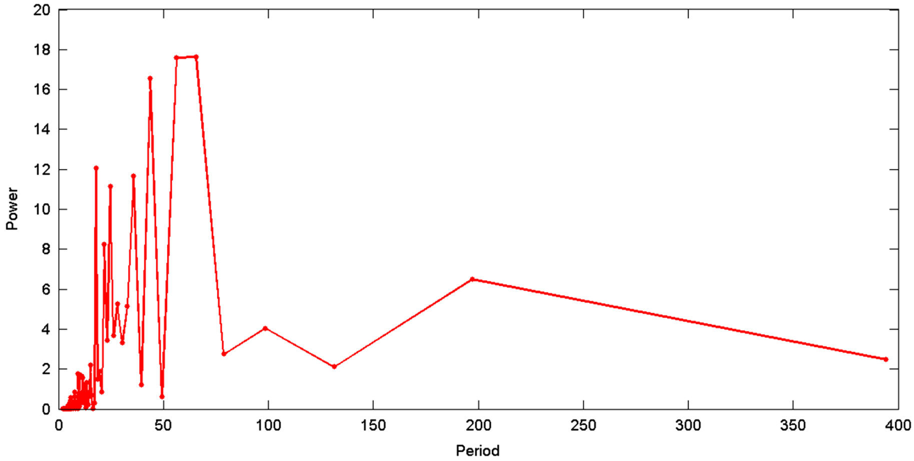

FIGURE 5 Frequency spectrum of PCTI 1982 to 2014 [Colour figure can be viewed at wileyonlinelibrary.com]

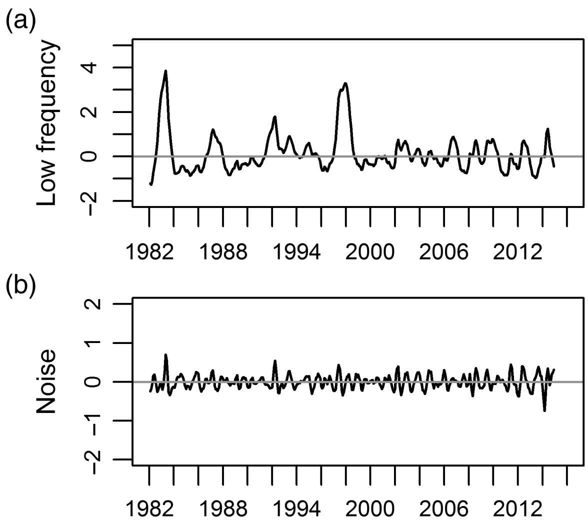

FIGURE 6 PCTI signal decomposition: (a) low frequency signal and (b) noise from 1982 to 2014

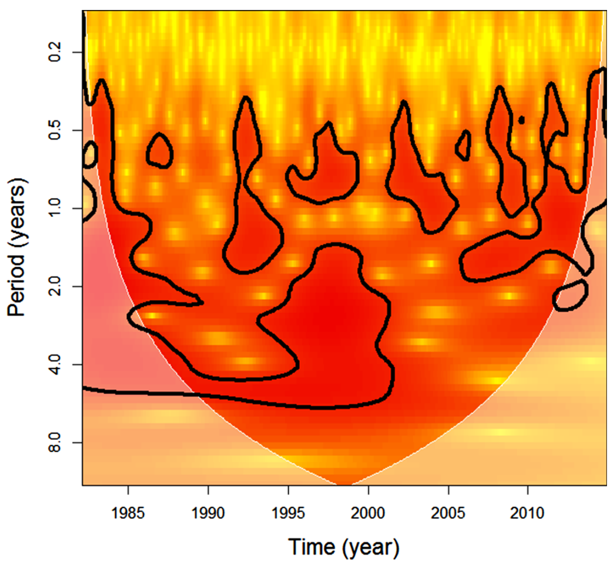

FIGURE 7 Wavelet spectrum of PCTI from 1982 to 2014 [Colour figure can be viewed at wileyonlinelibrary.com]

TABLE 3 Cross table of warm and cold periods between ONI and PCTI from 1982 to 2014

		PCTI			
		Cold	Neutral	Warm	Total
ONI	Cold	6	0	0	6
	Neutral	6	21	4	31
	Warm	0	1	8	9
	Total	12	22	12	46

TABLE 4 Cross table of warm and cold periods between PCTI and SN1 + 2 from 1982 to 2014

		SN1 + 2			
		Cold	Neutral	Warm	Total
PCTI	Cold	7	5	0	12
	Neutral	0	20	2	22
	Warm	0	0	12	12
	Total	7	25	14	46

TABLE 5 Cross table of warm and cold periods between ONI and SN1 + 2 from 1982 to 2014

		SN1 + 2			
		Cold	Neutral	Warm	Total
ONI	Cold	5	1	0	6
	Neutral	2	24	5	31
	Warm	0	0	9	9
	Total	7	25	14	46

depth off PUE was associated to a warm (cold) period of PCTI.

4 | DISCUSSION

The PCTI was developed to detect warm and cold periods in the PUE, using SVD analysis, often used in climate studies (Von Storch & Zwiers, 1999). The PCTI better represents PUE conditions, because in addition to ENSO effects, it captures a significant part of the upwelling variability; it

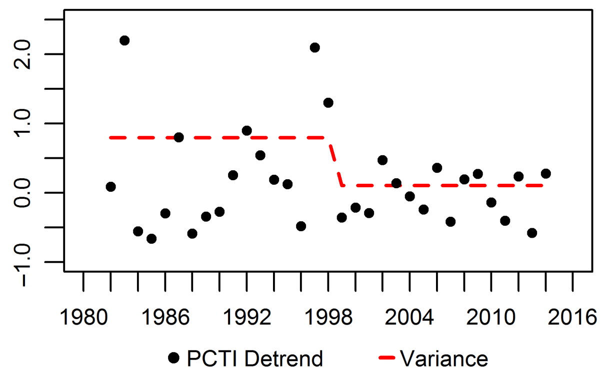

FIGURE 8 Regime shift analysis of PCTI from 1982 to 2014 [Colour figure can be viewed at wileyonlinelibrary.com]

is based on temporally continuous satellite SST data covering the whole area of the PUE, thus it cannot be replaced by in situ local information from coastal stations containing less comprehensive spatial integration, specially over the continental shelf.

Temporal variation of PCTI allowed to detect the duration of the thermal effects of EP and CP El Niño episodes. According to Yu and Kim (2013) during the period 1982–2014, two EP El Niño episodes were detected, five CP El Niño episodes and two Mixed type episodes. The thermal effects of EP El Niño 1982–1983 and 1997–1998, produced warm periods of 13 and 16 months, respectively, on the PUE according to PCTI. On the other hand, the thermal effects of CP El Niño 1991–1992, 1994–1995, 2002–2003 and 2009–2010, produced warm periods of 10, 4, 4 and 3 months, respectively, on the PUE according to PCTI. The CP El Niño 2004–2005 had no thermal effects on PUE.

It is noteworthy that warm periods of PCTI coincided with the peaks of the time series of in situ annual average of SST from piers along the Peruvian coast (figure 7 from Gutiérrez et al., 2011), in fact there is a significant correlation between SSTA from satellite data and in situ data at Chicama station (Figure 12).

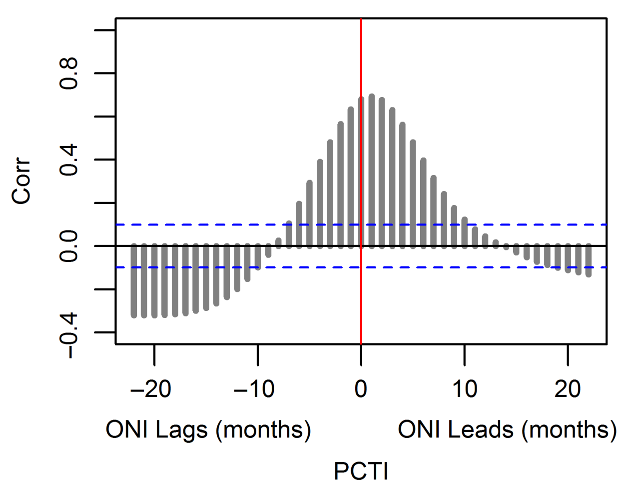

FIGURE 9 Cross-correlation function between PCTI and ONI [Colour figure can be viewed at wileyonlinelibrary.com]

The PCTI showed a regime shift in variance in 1999, which agreed with the regime shift of the PDO (Mantua, Hare, Zhang, Wallace, & Francis, 1997), which started a cold phase in 1999 (figure 6 from Newman et al., 2016; McPhaden, 2015). The warm phase of the PDO (1977–1998) is consistent with warm periods of PCTI, associated to EN 1982–1983, 1986–1987, 1991–1992, 1997–1998 events, which are considered of moderate to very strong intensity. On the other hand, the cold phase of the PDO agreed with warm periods of PCTI, associated to EN 2002–2003, 2004–2005, 2006–2007 and 2009–2010, considered as weak to moderate. It is noteworthy, that a decrease in the amplitude of PCTI and SST from piers along the Peruvian coast were seen since 1999 (figure 7 from Gutiérrez et al., 2011).

The change of variance of PCTI could be influenced by the SPA. An analysis of the differences in atmospheric pressure (Figure 10a,b) and wind stress (Figure 10c) from the periods 1982–1998 and 1999–2014 showed that the trade winds were more intense in the recent period. Stronger winds could produce more upwelling, counteracting thermal effects of EN episodes on the PUE, thus reducing the PCTI variability during 2000–2014 period. In addition, stronger trade winds along the coast of South America could facilitate the meridional transport of cold waters from Southern regions, also counteracting El Niño thermal effects on the PUE.

It is very important to explore in more detail five cases where PCTI and ONI did not match. In the first four cases, while warm periods occurred in the PUE, neutral conditions occurred in the EPO. In the first case, an EN condition was developing in the EPO which could have influenced the warm event in the PUE (March and September 1993), however possibly due to the passage of upwelling Kelvin waves (Boulanger & Menkes, 1995) EN conditions did not become an EN episode. In the second case, during the neutral phase previous to EN episode 2009–2010, downwelling Kelvin waves generated (L'Heureux, Bell, & Halpert, 2009) a warm event in the PUE (July and September 2008). In the third and fourth cases, an EN condition was developing in the EPO and the passage of downwelling Kelvin waves (Halpert, Bell, & L'Heureux, 2013; L'Heureux, Halpert, & Bell, 2015) generated warm periods in the PUE (May to August 2012 and May to July 2014), however due to the lack of westerly wind bursts, EN conditions did not evolved to an EN episode (Menkes et al., 2014).

In the fifth case, while a warm episode occurred in the EPO (Jul 2004 to April 2005), a neutral condition occurred in the PUE, because the CP El Niño 2004–2005 did not displayed an eastward warm pool displacement to the PUE.

There were also differences between SN1 + 2 and PTCI conditions, probably because N1 + 2 area is more

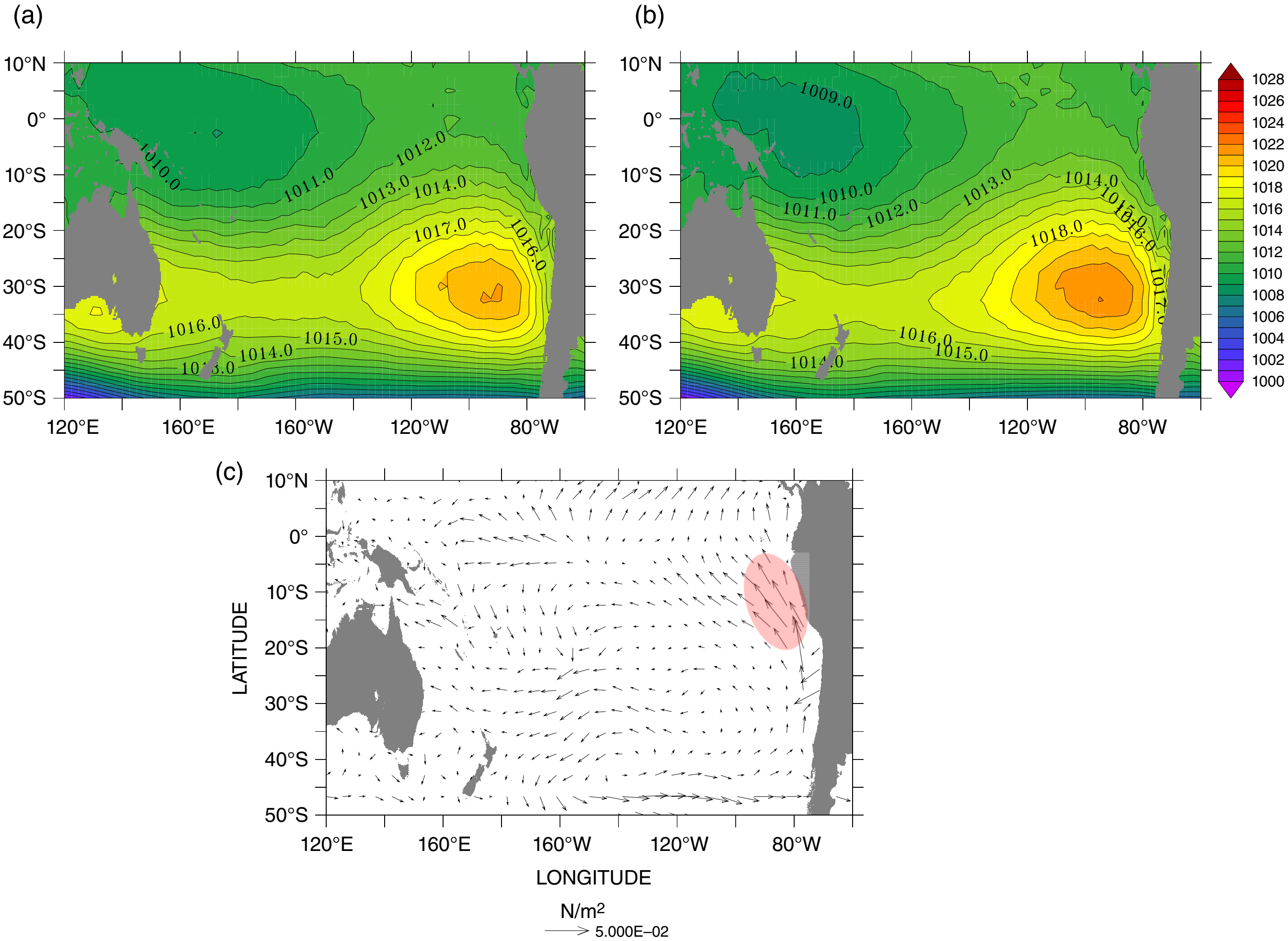

FIGURE 10 (a) Average of sea level atmospheric pressure (hPa) for 1982–1998, (b) 1999–2014 from NCEP-NCAR Reanalysis-1 and (c) stress winds vector difference (N/m^2) of the periods 1999–2014 and 1982–1998 from NCEP-DOE Reanalysis-2 [Colour figure can be viewed at wileyonlinelibrary.com]

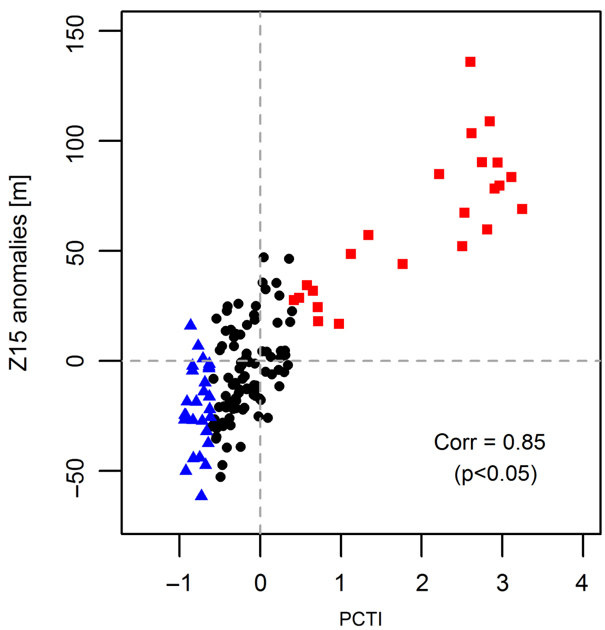

FIGURE 11 Correlation between time series of PCTI and Z15 anomalies from 1982 to 2008. Squares (triangles) points indicate Z15 anomalies associated to warm (cold) periods of PCTI [Colour figure can be viewed at wileyonlinelibrary.com]

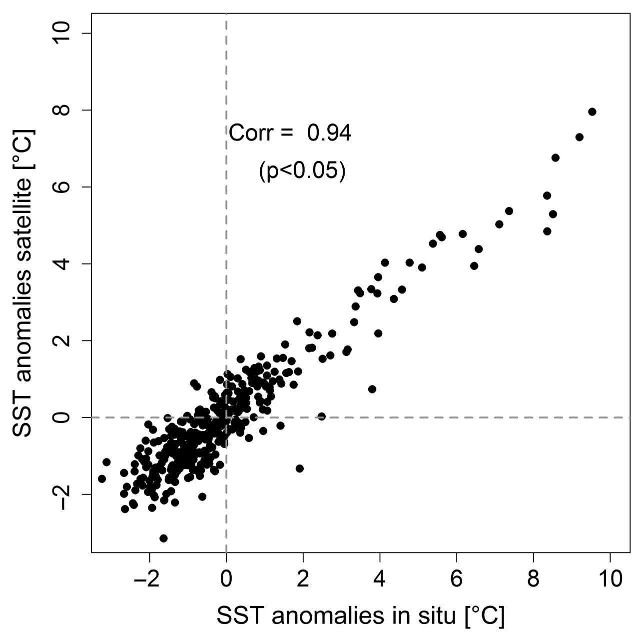

FIGURE 12 Comparison between sea surface temperature anomalies of satellite and in situ data in Chicama from 1982 to 2014

influenced by the passage of downwelling Kelvin waves than more coastal area of PUE. In two cases, while warm periods occurred in the Niño 1 + 2 region (November 2003 to January 2004 and October to December 2004), neutral periods occurred in the PUE. On the other hand, in five cases cold periods occurred in the PUE, while neutral periods occurred in the Niño 1 + 2 region. In one case, a cold period occurred in the PUE (February and April 1982) possibly due to intensification of alongshore winds, while a neutral period occurred in the Niño 1 + 2 region. Finally, in three cases, cold periods occurred in the PUE (April to June 1999, April to July 2004, September to November 2005 and December 2008 to March 2009), while neutral periods occurred in the Niño 1 + 2 region, possibly due to increase of alongshore winds associated to an intensification of the South Pacific Anticyclone.

Finally, it is worth mentioning that El Niño Phenomenon National Study ("ENFEN"), a Peruvian National Committee in charge of monitoring ENSO effects, has been using the SN1 + 2 index as the "Coastal Index of El Niño" ("ICEN" in Spanish) to monitor warm and cold anomalous periods off the Peruvian coast (ENFEN, 2012). However, ICEN has a limited spatial representativity, because its latitudinal range spans only from 0°S to 10°S and it has a coarse spatial resolution of 2°, these limitations were overcome by PCTI.

5 | CONCLUSIONS AND RECOMMENDATIONS

A PCTI was developed to represent the interannual variation of SST in the PUE. The added value of PCTI lies in the better description of the PUE compared to other indexes, because it covers most of the Peruvian area in the continental shelf, therefore including the thermal variability of the coastal upwelling, combined with the influence of EN and LN episodes.

The PCTI is the 3 month running average of the first normalized PC of the SSTA of the PUE, and represented 87.7% of total variance of SSTA, with a positive asymmetry in its frequency distribution. Between 1982 and 2014, the PCTI detected 12 warm periods and 16 cold periods in the PUE. The PCTI showed a linear trend component, a low frequency component and a noise component, with 1.5%, 94.5% and 4% contributions to total variance, respectively. Wavelet analysis of the PCTI showed the greatest variability in periods between 0.4 and 6 years, with significant peaks between the years 1996–1999.

Sequential analysis detected a regime shift of PCTI in 1999, with a variance decreasing from 1982–1998 to 1999–2014, which agreed with the transition phase of the PDO, which started a cold phase in 1999. The decrease of variance of the PCTI could be linked to the increase of the local wind associated with a higher intensity of the average state of South Pacific Anticyclone during the last 30 years that could have strengthened the upwelling and counteracted the intensity of warm periods in the PUE.

The comparison of indexes allowed to detect four cases where neutral conditions occurred in the EPO while warm periods occurred in the PUE (1993, 2008, 2012 and 2014); and one case where a warm episode occurred in the EPO (2004–2005) while a neutral condition occurred in the PUE.

As a recommendation, in this work we considered a fixed the boundary of the upwelling area, as the maximum zonal gradient of the annual SST, that separate coastal and oceanic waters. We suggest to explore a dynamical boundary of the upwelling area, as the maximum zonal gradient of each month of the climatology of SST.

ACKNOWLEDGEMENTS

This publication was carried out with the support of the IRD—JEAI EMACEP (Quantitative Marine Ecology of the Peruvian Upwelling Ecosystem) and The LMI DISCOH ("Dynamics of the Humboldt Currents System"). The authors wish to thank Vincent Echevin and François Colas from LOCEAN (IRD, France) for their valuable comments.

ORCID

C. Quispe-Ccalluari http://orcid.org/0000-0001-6465-2081

REFERENCES

Amador, J. A., Alfaro, E. J., Lizano, O. G., & Magaña, V. O. (2006). Atmospheric forcing of the eastern tropical Pacific: A review. *Progress in Oceanography*, *69*, 101–142.

Arntz, W. E., & Fahrbach, E. (1996). *El Niño: Experimento Climático de la Naturaleza*. México D.F.: Fondo de Cultura Económica.

Bakun, A. (1990). Global climate change and intensification of coastal ocean upwelling. *Science*, *247*, 198–201.

Barber, R. T., & Chavez, F. P. (1983). Biological consequences of El Niño. *Science*, *222*, 1203–1210.

Belmadani, A., Echevin, V., Dewitte, B., & Colas, F. (2012). Equatorially forced intraseasonal propagations along the Peru-Chile coast and their relation with the nearshore eddy activity in 1992–2000: A modelling study. *Journal of Geophysical Research*, *117*, C04025. https://doi.org/10.1029/2011JC007848

Boulanger, J.-P., & Menkes, C. (1995). Propagation and reflection of long equatorial waves in the Pacific Ocean during the 1992-1993 El Niño. *Journal of Geophysical Research*, *100*(C12), 25041–25059. https://doi.org/10.1029/95JC02956

Cai, W., Santoso, A., Wang, G., Weller, E., Wu, L., & Ashok, K. (2014). Increased frequency of extreme Indian Ocean Dipole events due to greenhouse warming. *Nature*, *510*, 254–258.

Camayo, R., & Campos, E. J. D. (2006). Application of wavelet transform in the study of coastal trapped waves off the west coast of South America. *Geophysical Research Letters*, *33*, L22601. https://doi.org/10.1029/2006GL026395

Capotondi, A., Wittenberg, A. T., Newman, M., Di Lorenzo, E., Yu, J.-Y., Braconnot, P., … Yeh, S.-W. (2015). Understanding ENSO diversity. *Bulletin of the American Meteorological Society*, *96*, 921–938. https://doi.org/10.1175/BAMS-D-13-00117.1

Chatfield, C. (1996). *The analysis of times series: An introduction* (5th ed.). Chapman & Hall, CRC Press: Boca Raton, FL.

Chavez, F. P., Bertrand, A., Guevara-Carrasco, R., Soler, P., & Csirke, P. (2008). The northern Humboldt Current System: Brief history, present status and a view towards the future. *Progress in Oceanography*, *79*, 95–105. https://doi.org/10.1016/j.pocean.2008.10.012

Chavez, F. P., Ryan, J., Lluch-Cota, S., & Ñiquen, M. (2003). From Anchovies to Sardines and back: Multidecadal change in the Pacific Ocean. *Science*, *299*, 217–221.

Colas, F., Capet, X., McWilliams, J. C., & Shchepetkin, A. (2008). 1997-98 el Niño off Peru: A numerical study. *Progress in Oceanography*, *79*, 138–155. https://doi.org/10.1016/j.pocean.2008.10.015

Dewitte, B., Vazquez-Cuervo, J., Goubanova, K., Illig, S., Takahashi, K., Cambon, G., … Ortlieb, L. (2012). Change in El Niño flavours over 1958–2008: Implications for the long-term trend of the upwelling off Peru. *Deep Sea Research Part II: Topical Studies in Oceanography*, *77-80*, 143–156. https://doi.org/10.1016/j.dsr2.2012.04.011

Di Lorenzo, E., Combes, V., Keister, J. E., Strub, P. T., Thomas, A. C., Franks, P. J. S., … Parada, C. (2013). Synthesis of Pacific Ocean climate and ecosystem dynamics. *Oceanography*, *26*(4), 68–81. https://doi.org/10.5670/oceanog.2013.76

Echevin, V., Goubanova, K., Belmadani, A., & Dewitte, B. (2012). Sensitivity of the Humboldt Current system to global warming: A downscaling experiment of the IPSL-CM4 model. *Climate Dynamics*, *38*, 761–774.

Emery, W. J., & Thomson, R. E. (2004). *Data analysis methods in physical oceanography* (2nd ed.). Elservier Science: Amsterdam, Netherlands.

ENFEN. (2017). *El Niño Costero 2017* (Informe Técnico Extraordinario N°001-2017). Lima, Perú (pp. 1–31). Retrieved from http://www.imarpe.pe/imarpe/archivos/informes/imarpe_inftco_informe__tecnico_extraordinario_001_2017.pdf

Espinoza-Morriberón, D., Echevin, V., Colas, F., Tam, J., Ledesma, J., Vásquez, L., & Graco, M. (2017). Impacts of El Niño events on the Peruvian upwelling system productivity. *Journal of Geophysical Research. Oceans*, *122*, 5423–5444. https://doi.org/10.1002/2016JC012439

Gutiérrez, D., Bertrand, B., Wosnitza-Mendo, C., Dewitte, B., Purca, S., Peña, C., … Guevara-Carrasco, R. (2011). Sensibilidad del sistema de afloramiento costero del Perú al cambio climático e implicancias ecológicas. *Revista Peruana Geo-Atmosférica*, *3*, 1–24.

Halpert, M., Bell, G. D., & L'Heureux, M. (2013). [Tropics] ENSO and the tropical Pacific [in "state of the climate in 2012"]. *Bulletin of the American Meteorological Society*, *94*(8), S79–S82.

Illig, S., Dewitte, B., Goubanova, K., Cambon, G., Boucharel, J., Monetti, F., … Flores, R. (2014). Forcing mechanisms of intraseasonal SST variability off Central Peru in 2000-2008. *Journal of Geophysical Research. Oceans*, *119*, 3548–3573. https://doi.org/10.1002/2013JC009779

Kao, H.-Y., & Yu, J.-Y. (2009). Contrasting eastern-Pacific and central-Pacific. Types of El Niño. *Journal of Climate*, *22*, 615–632.

Karnauskas, K. B. (2013). Can we distinguish canonical El Niño from Modoki? *Geophysical Research Letters*, *40*, 5246–5251. https://doi.org/10.1002/grl.51007

Klein, S. A., & Hartmann, D. L. (1993). The seasonal cycle of low stratiform cloud. *Journal of Climate*, *6*, 1587–1606. https://doi.org/10.1175/1520-0442(1993)006<1587:TSCOLS>2.0.CO;2

Kosaka, Y., & Xie, S.-P. (2013). Recent global-warming hiatus tied to equatorial Pacific surface cooling. *Nature*, *501*, 403–407. https://doi.org/10.1038/nature12534

Kug, J.-S., Jin, F.-F., & An, S.-I. (2009). Two types of El Niño events: Cold tongue El Niño and warm pool El Niño. *Journal of Climate*, *22*, 1499–1515.

L'Heureux, M., Bell, G., & Halpert, M. (2009). ENSO and the tropical Pacific [in "state of the climate in 2008"]. *Bulletin of the American Meteorological Society*, *90*(8), S75–S79.

Lee, T., & McPhaden, M. J. (2010). Increasing intensity of El Niño in the central equatorial Pacific. *Geophysical Research Letters*, *37*, L14603. https://doi.org/10.1029/2010GL044007

L'Heureux, M., Halpert, M., & Bell, G. D. (2015). ENSO and the tropical Pacific [in "state of the climate in 2014"]. *Bulletin of the American Meteorological Society*, *96*(7), S91–S92.

Liu, Y., Liang, X. S., & Weisberg, R. H. (2007). Rectification of the bias in the wavelet power spectrum. *Journal of Atmospheric and Oceanic Technology*, *24*, 2093–2102. https://doi.org/10.1175/2007JTECHO511.1

Mantua, N. J., Hare, S. R., Zhang, Y., Wallace, J. M., & Francis, R. C. (1997). A Pacific interdecadal climate oscillation with impacts on salmon production. *Bulletin of the American Meteorological Society*, *78*, 1069–1079. https://doi.org/10.1175/1520-0477(1997)078,1069:APICOW.2.0.CO;2

McPhaden, M. J. (2002). El Niño and La Niña: Causes and global consequences. In *Encyclopedia of global environmental change* (Vol. *1*, pp. 353–370). Chichester, England: John Wiley and Sons.

McPhaden, M. J. (2015). Playing hide and seek with El Niño. *Nature Climate Change*, *5*, 791–795. https://doi.org/10.1038/nclimate2775

McPhaden, M. J., Zebiak, Z. E., & Glantz, M. H. (2006). ENSO as an integrating concept in earth science. *Science*, *314*, 1740–1745.

Menkes, C. E., Lengaigne, M., Vialard, J., Puy, M., Marchesiello, P., Cravatte, S., & Cambon, G. (2014). About the role of westerly wind events in the possible development of an El Niño in 2014. *Geophysical Research Letters*, *41*, 6476–6483. https://doi.org/10.1002/2014GL061186

Newman, M., Alexander, M. A., Ault, T. R., Cobb, K. M., Deser, C., Di Lorenzo, E., … Smith, C. A. (2016). The Pacific Decadal Oscillation, revisited. *Journal of Climate*, *29*, 4399–4427. https://doi.org/10.1175/JCLI-D-15-0508.1

NOAA Magazine. (2003, September 30). *NOAA gets U.S. consensus for El Niño/La Niña index, definitions.* Retrieved from http://www.noaanews.noaa.gov/stories/s2095.htm

NOAA. (2015, October 15). *CPC: Oceanic EL Niño Index.* Retrieved from http://www.cpc.ncep.noaa.gov/products/analysis_monitoring/ensostuff/ensoyears.shtml

Pennington, J. T., Mahoney, K. L., Kuwahara, V. S., Kolber, D. D., Calienes, R., & Chavez, F. P. (2006). Primary production in the eastern tropical Pacific: A review. *Progress in Oceanography*, *69*, 285–317.

R Core Team. (2016). *R: A language and environment for statistical computing.* Vienna, Austria: R Foundation for Statistical Computing. Retrieved from https://www.R-project.org/

Rahn, D., & Garreaud, R. (2014). A synoptic climatology of the near-surface wind along the west coast of South America. *International Journal of Climatology*, *34*, 780–792. https://doi.org/10.1002/joc.3724

Ramírez, I. J., & Briones, F. (2017). Understanding the El Niño Costero of 2017: The definition problem and challenges of climate forecasting and disaster responses. *International Journal of Disaster Risk Science*, *8*, 489–492. https://doi.org/10.1007/s13753-017-0151-8

Rasmusson, E. M., & Carpenter, T. H. (1982). Variations in Tropical Sea surface temperature and surface wind fields associated with the Southern Oscillation/El Niño. *Monthly Weather Review*, *110*, 354–384.

Reynolds, R. W., Smith, T. M., Liu, C., Chelton, D. B., Casey, K. S., & SchlaxM, G. (2007). Daily high-resolution blended analyses for sea surface temperature. *Journal of Climate*, *20*, 5473–5496.

Rodionov, S. (2004). A sequential algorithm for testing climate regime shifts. *Geophysical Research Letters*, *31*, L09204. https://doi.org/10.1029/2004GL019448

Smith, T. M., Reynolds, R. W., Peterson, T. C., & Lawrimore, J. (2008). Improvements NOAAs historical merged Land–Ocean temp analysis (1880–2006). *Journal of Climate*, *21*, 2283–2296.

Takahashi, K., & Martinez, A. G. (2017). The very strong coastal El Niño in 1925 in the far-eastern Pacific. *Climate Dynamics*. https://doi.org/10.1007/s00382-017-3702-1

Takahashi, K., Montecinos, A., Goubanova, K., & Dewitte, B. (2011). ENSO regimes: Reinterpreting the canonical and Modoki El Niño. *Geophysical Research Letters*, *38*, L10704. https://doi.org/10.1029/2011GL047364

Torrence, C., & Compo, G. P. (1998). A practical guide to wavelet analysis. *Bulletin of the American Meteorological Society*, *79*, 61–78.

Trenberth, K. E., Branstator, G. W., Karoly, D., Kumar, A., Lau, N. G., & Ropelewski, C. (1998). Progress during TOGA in understanding and modeling global teleconnections associated with tropical sea surface temperatures. *Journal of Geophysical Research*, *103*, 14291–14324.

U.S. CLIVAR Report. (2013). *ENSO Diversity Working Group: Report on the ENSO diversity workshop* (US CLIVAR Report No. 2011-1). US CLIVAR Project Office, 20 pp. Retrieved from http://www.usclivar.org/sites/default/files/meetings/ENSO_Diversity_Workshop_Report.pdf

Venables, W. N., & Ripley, B. D. (2002). *Modern applied statistics with S* (4th ed.). New York, NY: Springer. isbn:0-387-95457-0.

Von Storch, H., & Zwiers, F. W. (1999). *Statistical analysis in climate research*. Cambridge, MA: Cambridge University Press.

Xu, Y., Chaia, F., Roseb, K. A., Ñiquen, M., & Chavez, F. P. (2013). Environmental influences on the interannual variation and spatial distribution of Peruvian anchovy (Engraulis ringens) population dynamics from 1991 to 2007: A three-dimensional modeling study. *Ecological Modelling*, *264*, 64–82. https://doi.org/10.1016/j.ecolmodel.2013.01.009

Yu, J.-Y., & Kim, S. T. (2013). Identifying the types of major El Niño events since 1870. *International Journal of Climatology*, *33*, 2105–2112. https://doi.org/10.1002/joc.3575

Zuta, S., & Guillén, O. (1970). Oceanografía de las aguas costeras del Perú. *Boletin Instituto del Mar del Perú*, *2*, 157–324.

How to cite this article: Quispe-Ccalluari C, Tam J, Demarcq H, et al. An index of coastal thermal effects of El Niño Southern Oscillation on the Peruvian Upwelling Ecosystem. *Int J Climatol*. 2018;1–11. https://doi.org/10.1002/joc.5493